



Whole exome sequencing identifies a rare variant in *DAAM2* as a potential candidate in idiopathic pulmonary ossification

Sheng-Wen Sun, Mei Zhou, Long Chen, Jiang-Hua Wu, Zhao-Ji Meng, Shuai-Ying Miao, Hong-Li Han, Chen-Chen Zhu, Xian-Zhi Xiong

Department of Respiratory Medicine, Union Hospital, Tongji Medical College, Huazhong University of Science and Technology, Wuhan 430022, China

Contributions: (I) Conception and design: SW Sun, XZ Xiong; (II) Administrative support: XZ Xiong, M Zhou; (III) Provision of study materials or patients: M Zhou, SY Miao; (IV) Collection and assembly of data: ZJ Meng, JH Wu; (V) Data analysis and interpretation: SW Sun, L Chen, HL Han, CC Zhu; (VI) Manuscript writing: All authors; (VII) Final approval of manuscript: All authors.

Correspondence to: Xian-Zhi Xiong, PhD. Department of Respiratory Medicine, Union Hospital, Tongji Medical College, Huazhong University of Science and Technology, 1277 Jiefang Avenue, Wuhan 430022, China. Email: xxz0508@hust.edu.cn.

Background: Diffuse pulmonary ossification (DPO) is a rare disease characterized by bone tissue formation in the lung. DPO can be classified into idiopathic pulmonary ossification (IPO) and secondary pulmonary ossification. Cases with no identified etiology are classified as IPO. Variants of dishevelled associated activator of morphogenesis 2 (*DAAM2*) have been reported to be involved in the bone-resorption of osteoclasts.

Methods: Whole exome sequencing (WES) was used on samples from a patient with IPO and his healthy parents. The effects of all variants were determined using functional predictors (PolyPhen-2, SIFT, FATHMM and MutationTaster); variants existing only in the patient were further screened compared with his healthy parents.

Results: Forty deleterious variants, including 25 single nucleotide variants (SNVs) and 15 insertions and deletions (indels), were identified by WES. Finally, *DAAM2* (c.G2960T;p.R987L) was screened by pathway analysis.

Conclusions: We identified a novel variant of *DAAM2* (c.G2960T;p.R987L) that might participate in the disease process of IPO.

Keywords: Idiopathic pulmonary ossification (IPO); whole exome sequencing (WES); dishevelled associated activator of morphogenesis 2 (*DAAM2*); heterotopic ossification, genetic variants

Submitted Feb 14, 2019. Accepted for publication May 29, 2019.

doi: 10.21037/atm.2019.06.14

View this article at: <http://dx.doi.org/10.21037/atm.2019.06.14>

Introduction

First described in 1864, diffuse pulmonary ossification (DPO) is characterized by unusual widespread bony metaplastic formation in the lung. In general, DPO is found in elderly men over the age of over 70 years, and the estimated incidence rate of DPO is in the range of 0.16–0.5% (1,2). Pulmonary ossification is not found exclusively in humans: it has also been described in animals such as dogs (3). In general, idiopathic pulmonary ossification (IPO)

is an uncommon and asymptomatic disorder with unknown etiology, while secondary pulmonary ossification may be observed in cases of chronic bronchitis, interstitial lung disease, tuberculosis, and lung cancer (4–7). In addition, from a histological point of view, DPO has two distinct forms: dendriform pulmonary ossification and nodular pulmonary ossification. The former is less common and is characterized by branching along terminal airways with occasional islands of marrow, whereas nodular pulmonary ossification tends to be more circumscribed and situated in

the alveolar spaces (8). However, this classification method may be of little use in determining etiology.

IPO usually presents an indolent and chronic course accompanied by slightly restrictive pulmonary ventilation dysfunction. IPO is so rare that it may be poorly diagnosed, and most cases have been diagnosed during autopsy (9). Laboratory investigations, including serum calcium and phosphorus levels, were within normal in the identified cases (9,10). No effective treatment for IPO has been found. Some studies have reported that low-calcium diets, calcium binding drugs, steroids, and bisphosphonates failed to show the expected results in terms of inhibiting ossification (11).

Whole exome sequencing (WES), or next-generation sequencing, has been successfully applied to detect potential variants in the exome for Mendelian diseases and orphan diseases. Because of WES, great advancements in understanding the etiology and improving the treatment of rare diseases have been made (12).

Approximately 20 IPO cases have previously been reported (13-29). Among these cases, interestingly, two familial clusters of cases were proposed, which strongly suggested a genetic influence in the pathogenesis of IPO (15,22). However, due to the low morbidity and low rate of diagnosis of IPO, genetic findings regarding this rare disease are still non-existent.

BMP/Smads, Wnt/ β -catenin and OPG/RANKL/RANK signalling pathways have been well studied in bone metabolism. According to a previous study, the dishevelled associated activator of morphogenesis 2 (*DAAM2*), an effector of the Wnt signalling pathway, was reported to promote osteoclastic bone-resorbing (30). Variants of *DAAM2* might lead to abnormal bone build-up.

IPO may be a multifactorial disease: it is unclear whether a genetic influence is involved in the pathogenesis of IPO, and the inheritance pattern has not been determined. According to the previous literature and the characteristics of our patient, IPO may be likely caused by *de novo* variants or an autosomal recessive genetic disease. Therefore, WES was conducted on a patient with IPO to explore potential causative variants of this rare disease and to provide genetic insights into its etiology and treatment.

Methods

Patient's clinical information

A 28-year-old male patient who was a non-smoker presented to our respiratory unit with dyspnea on exertion.

He had no cough, hemoptysis, chest pain, fever or weight loss. He had no significant environmental or occupational exposure, epidemiological history, or family history of respiratory diseases. He once suffered from childhood pneumonia. Chest radiography from 2 years prior reportedly showed diffuse shadows. Crepitation could not be heard during a physical examination. Laboratory findings showed that according to a routine blood examination, levels of rheumatoid factors, antineutrophil cytoplasmic antibodies (ANCA) and anti-extractable nuclear antigen antibodies (ENA) were within normal ranges. A high-resolution computed tomography (HRCT) scan showed pulmonary interstitial lesions (*Figure 1A,B*). Pulmonary function testing showed mildly restrictive pulmonary ventilation dysfunction, small airway dysfunction disorders and reduced diffusion (*Table S1*). Thereafter, the patient received no treatment for 2 years; later CT scans (*Figure 1C,D*) did not show significant changes, while other tests revealed slightly worsened pulmonary function (*Table S1*). The proband's parents had normal lung function, X-ray findings and clinical examinations.

WES and variant prioritization

Whole blood samples were obtained from the patient and his healthy parents. WES was performed using an Illumina HiSeq X-ten system by the HaploX Genomics Centre. Burrows-Wheeler Aligner (BWA) was used to generate alignment with the human genome reference sequence (hg 19). Subsequently, variants, including single nucleotide variants (SNVs) and small insertions and deletions (indels), were identified by the Genome Analysis Toolkit (GATK). Circos was used to describe the SNV/indel information. Variant annotation was performed by ANNOVAR [2015-03-22]. ESP6500siv2 (mutation frequency <0.01) and the 1000 Genomes database (mutation frequency <0.01) were used to filter low frequency variants. Functional predictors of variants were tested by PolyPhen-2 (Polyphen2_pred = "D" or "P"; "D" means probably damaging, "P" means possibly damaging), the Stanford Information Filtering Tool (SIFT_score <0.05, indicting a variant is deleterious), FATHMM (FATHMM_pred = "D"; "D" means disease_causing) and MutationTaster (Mutationtaster_pred = "A" or "D"; "A" means disease_causing_automatic, "D" means disease_causing); SNVs with deleterious predictions by SIFT, PolyPhen-2 and MutationTaster were considered for the next step (31-33); for indels, FATHMM and MutationTaster were used (33,34).

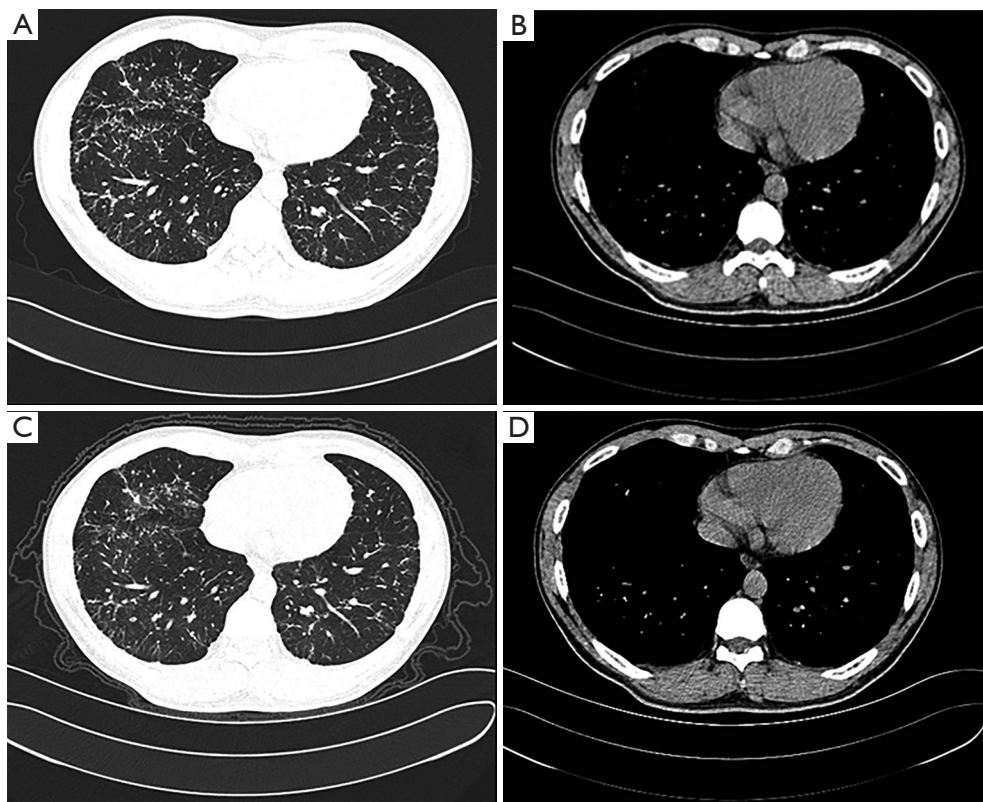


Figure 1 High-resolution computed tomography (HRCT) images of the proband. Lung windows and mediastinal windows of HRCT images of the chest showing there is no apparent progression of lung lesions over 2 years. (A,B) CT images of 2015-05-12; (C,D) images of 2017-07-12.

On one hand, to screen the variants that were homozygous in the proband but heterozygous in the patients. On the other hand, we sought to identify the variants that were present in the proband but not in his healthy parents (*Figure S1*).

Results

Diagnosis of IPO

IPO is an uncommon and asymptomatic disorder that may be poorly diagnosed. The key to its diagnosis is the presence of heterotic bone tissue formation in the lung and the exclusion of underlying secondary etiologies. Histopathology (*Figure 2*) of a surgical lung biopsy specimen from our patient showed bone metaplasia formation with partial bone marrow. Serum calcium, serum phosphate, vitamin D and parathyroid hormone (PTH) levels were within normal ranges. The cardiac ultrasound did not show any abnormalities. A comprehensive analysis of

the test results demonstrated that our evidence supported the diagnosis of IPO.

Deleterious genes filtered by genetic analysis

WES generated a yield of 11–16 Gb of data for each individual; 92% of the target region covered a depth of more than 10×, and the average coverage depth exceeded 200×, which met the analysis requirements. Overall, 55,225 SNVs and 7,007 indels were selected after alignment and variant calling. An overview of the information regarding the variants containing SNVs/indels on each chromosome is shown in *Figure S2*. Through exome region (including exonic, splicing, ncRNA, UTR-3 and UTR-5) filtering, 24,185 variants were found, including 23,427 SNVs and 758 indels. By selecting non-synonymous, stop-gain, stop-loss, frame-shift insertion, frame-shift deletion and missense variants, 11,223 SNVs and 263 indels were further prioritized. By filtering low frequency variants, 1,691 SNVs

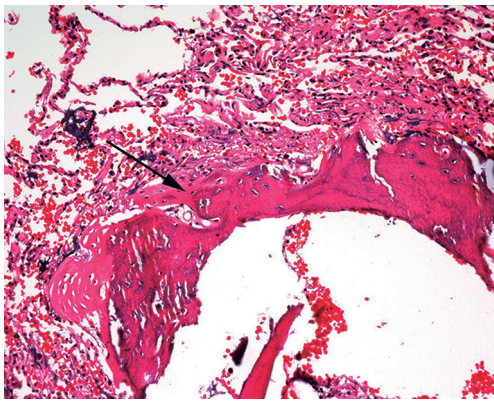


Figure 2 Histopathology of lung biopsy. Histology of the pulmonary lesions (arrow) showing bone tissue formation in the lung (haematoxylin and eosin staining, original magnification $\times 200$).

and 137 indels were selected. Next, 333 variants (196 SNVs and 137 indels) were filtered by functional predictors. Unfortunately, no variants were screened following an autosomal recessive inheritance. However, 40 potential *de novo* variants, including 25 SNVs, and 15 indels were identified in the patient. The filtering process applied to the variants is shown in *Figure S3*.

Pathway analysis of the 40 deleterious variants

The 40 identified variants are listed in *Table S2*. As BMP/Smads, Wnt/ β -catenin, and OPG/RANKL/RANK were the best-studied signalling pathways that affect bone metabolism, we chose variants of genes encoding proteins involved in the above pathways. The literature indicates that *DAAM2* mediates the Wnt5a/ β -catenin signalling pathway (35), which promotes the bone-resorption of osteoclasts. These results suggested that variants of *DAAM2* can cause abnormalities in bone metabolism, leading to IPO.

Discussion

In general, IPO is associated with longstanding pulmonary injury and has unknown specific clinical implications and pathological significance. Therefore, the identification of the genetic variants involved is essential for disease identification and treatment. Herein, we diagnosed a rare case of IPO by lung biopsy, and further WES identified a *de novo* variant of *DAAM2* (c.G2960T;p.R987L) in the proband, which may be associated with IPO.

We propose that WES may be a potential method of

molecularly diagnosing IPO patients in the clinical setting. However, several genes, including ubiquitin-specific peptidase 17-like family member 8 (*USP17L8*), gamma-glutamyltransferase light chain 2 (*GGTLC2*), mucin 3A (*MUC3A*), CTAGE family, member 6 (*CTAGE6*), SCOP-spondin (*SSPO*), proline-rich protein BstNI subfamily 3 (*PRB3*), SLAIN motif family, member 1 (*SLAIN1*) and axonemal central pair apparatus protein (*HYDIN*), have not been extensively studied, and both their functions and the significance of their variants should be further evaluated.

DAAM2 may play an important role in the occurrence and development of lung, kidney, colorectal and glioma tumours (36-39). *DAAM2* was found to be elevated in the acute phase of Guillain-Barre syndrome through the Wnt signalling pathway (40). *DAAM2* was reported to regulate heart morphogenesis combining with *DAAM1* (41). A previous study demonstrated that *DAAM2* also regulated the development of CNS via Wnt signalling (35). In our study, we suggest that *DAAM2* may regulate bone-resorption in the lung, and dysfunction of *DAAM2* (c.G2960T;p.R987L) may be responsible for the occurrence of heterotopic ossification in the lung. It appears that the other 39 candidate variants we found may also play roles in bone metabolism, and the exact mechanisms need to be further studied.

A literature review indicates that IPO is associated with a myriad of pathogenesis pathways. According to a study by Chan *et al.*, pulmonary ossification is the consequence of a series of pathophysiological changes, including the degeneration of the arterial media and the inflammation and hyalinization of the perivascular tissue, and it may have a close relationship with dystrophic pulmonary calcification (11). Kawakami and colleagues suggested that certain conditions such as tissue acidosis caused by hypoxia and capillary congestion might play roles in the formation of osseous tissue (4). Some have suggested that chronic intra-alveolar hemorrhage appeared to be associated with subsequent fibrosis and ossification (42). However, tissue damage is believed to be the most important triggering factor, because it can induce the precipitation of calcium salt, the activation of alkaline phosphatase and the production of profibrogenic cytokines in an alkaline environment (43). The transforming growth factor- β (TGF- β) superfamily was reported to play a role in metaplastic bone formation by stimulating osteoblast and chondrocyte proliferation (44). Interleukin-1 and interleukin-4 have also been shown to induce bone formation (11,45,46).

IPO represents a rare form of heterotopic ossification,

and great achievements have been made in genetic research on heterotopic ossification. Although several discoveries in the genetic basis for heterotopic ossification have been reported, its mechanism is still unclear. According to a report by Agarwal *et al.*, inhibition of Hif1 α (a mediator of cellular adaptation to hypoxia) can prevent heterotopic ossification in a mouse model (47). Mitchell *et al.* suggested that three candidate variants in ADRB2, TLR4 and CFH are associated with heterotopic ossification (48). SEMA3A was reported to play a role in neurogenic heterotopic ossification (49). However, ACVR1 and GNAS were not found in a mesenteric heterotopic ossification patient, although they were reported to have a potential connection to heterotopic ossification (50-52).

It should be noted that this study included WES results for only one IPO case; therefore, we may have missed potentially significant variants outside the exons and variants coding sequences, such as those in the promoter or other regulatory elements. However, this problem could be overcome by the additional genetic analysis of other patients with IPO. Although computational software that predicts deleterious effects of variants on protein function provides powerful evidence for screening candidate variants, these tools are not suitable for testing other types of variants, including copy number variations and fusions. In addition, we failed to provide proper treatment for the patient. It is believed that awareness and recognition of this rare disease can lead to further discoveries that would elucidate the mechanism and treatment of IPO.

Conclusions

In summary, we diagnosed a rare case of IPO and a *de novo* variant of *DAAM2* (c.G2960T:p.R987L) by WES that may participate in the progression of this rare disease. To our knowledge, our case represents the first report to evaluate the genetic mechanism of IPO by WES, and we hope that this study attracts more attention to IPO. We also want to stress the importance of lung biopsy or bronchial lung biopsy and genetic testing to identify the causes of and future therapy for IPO.

Acknowledgments

The authors would like to acknowledge Professor Xiu Nie and Doctor Jun Fan of our department and Professor Fan-Qin Meng of Nanjing Drum Tower Hospital and the Affiliated Hospital of Nanjing University Medical School

for their assistance with the pathology. We also would like to thank the patient and his parents for participating in this research.

Funding: This work was supported by the National Natural Science Foundation of China (No. 81370146, No. 8157010658 and No. 8150010542).

Footnote

Conflicts of Interest: The authors have no conflicts of interest to declare.

Ethical Statement: The study was approved by the Medical Ethics Committees of the Tongji Medical College of the Huazhong University of Science and Technology (No. 2015-101). All blood donors provided written informed consent before participating in this study.

References

1. Lara JF, Catroppo JF, Kim DU, et al. Dendriiform pulmonary ossification, a form of diffuse pulmonary ossification: report of a 26-year autopsy experience. *Arch Pathol Lab Med* 2005;129:348-53.
2. Tseung J, Duflo J. Diffuse pulmonary ossification: an uncommon incidental autopsy finding. *Pathology* 2006;38:45-8.
3. Kubba MAG. Pulmonary ossification and microlithiasis in a bitch with multicentric mammary tumors. *Open Vet J* 2017;7:273-6.
4. Kawakami Y, Abe S, Nishimura M, et al. Diffuse pulmonary ossification associated with chronic bronchitis. *Jpn J Med* 1987;26:409-12.
5. Trejo O, Xaubet A, Marin-Arguedas A, et al. Dendriiform pulmonary ossification associated with idiopathic pulmonary fibrosis. *Arch Bronconeumol* 2002;38:399-400.
6. Eum SY, Kong JH, Jeon BY, et al. Metaplastic ossification in the cartilage of the bronchus of a patient with chronic multi-drug resistant tuberculosis: a case report. *J Med Case Rep* 2010;4:156.
7. Aoki H, Nagase A, Fujiuchi S, et al. Expression of bone morphogenetic protein 2 in lung adenocarcinoma with ossification. *Kyobu Geka* 2014;67:1159-61.
8. Popelka CG, Kleinerman J. Diffuse pulmonary ossification. *Arch Intern Med* 1977;137:523-5.
9. Felson B, Schwarz J, Lukin RR, et al. Idiopathic pulmonary ossification. *Radiology* 1984;153:303-10.
10. Peros-Golubicic T, Tekavec-Trkanjec J. Diffuse pulmonary

- ossification: an unusual interstitial lung disease. *Curr Opin Pulm Med* 2008;14:488-92.
11. Chan ED, Morales DV, Welsh CH, et al. Calcium deposition with or without bone formation in the lung. *Am J Respir Crit Care Med* 2002;165:1654-69.
 12. Metzker ML. Sequencing technologies - the next generation. *Nat Rev Genet* 2010;11:31-46.
 13. Abe J, Oura H, Niikawa H, et al. Dendriiform pulmonary ossification: unusual cause of spontaneous pneumothorax. *Thorax* 2014;69:97-8.
 14. Ahari JE, Delaney M. Dendriiform pulmonary ossification: a clinical diagnosis with 14 year follow-up. *CHEST* 2007;132:701A.
 15. Azuma A, Miyamoto H, Enomoto T, et al. Familial clustering of dendriiform pulmonary ossification. *Sarcoidosis Vasc Diffuse Lung Dis* 2003;20:152-4.
 16. Bai P, Sun YC, Chen DN, et al. Idiopathic diffuse pulmonary ossification: a case report and review of the literature. *Zhonghua Jie He He Hu Xi Za Zhi* 2009;32:588-92.
 17. Bisceglia M, Chiaramonte A, Panniello G, et al. Selected case from the Arkadi M. Rywlin international pathology slide series: diffuse dendriiform pulmonary ossification: report of 2 cases with review of the literature. *Adv Anat Pathol* 2015;22:59-68.
 18. Fernandez-Bussy S, Labarca G, Pires Y, et al. Dendriiform pulmonary ossification. *Respir Care* 2015;60:e64-7.
 19. Gortenuiti G, Portuese A. Disseminated pulmonary ossification. *Eur J Radiol* 1985;5:14-6.
 20. Harvey NT, Heraganhally S, Au V, et al. Idiopathic diffuse dendriiform pulmonary ossification in a dental technician. *Pathology* 2012;44:363-5.
 21. Kato T, Ishikawa K, Kadoya M, et al. Spontaneous pneumothorax in a patient with dendriiform pulmonary ossification: report of a case. *Surg Today* 2012;42:903-8.
 22. Kinoshita Y, Mizuguchi I, Hidaka K, et al. Familial diffuse pulmonary ossification: A possible genetic disorder. *Respir Investig* 2017;55:79-82.
 23. Martinez JB, Ramos SG. Dendriiform pulmonary ossification. *Lancet* 2013;382:e22.
 24. Mizushima Y, Bando M, Hosono T, et al. A rare case of asymptomatic diffuse pulmonary ossification detected during a routine health examination. *Intern Med* 2012;51:2923-7.
 25. Ndimbie OK, Williams CR, Lee MW. Dendriiform pulmonary ossification. *Arch Pathol Lab Med* 1987;111:1062-4.
 26. Reddy TL, von der Thusen J, Walsh SL. Idiopathic dendriiform pulmonary ossification. *J Thorac Imaging* 2012;27:W108-10.
 27. Ryan CF, Flint JD, Muller NL. Idiopathic diffuse pulmonary ossification. *Thorax* 2004;59:1004.
 28. Tsai AP, English JC, Murphy D, et al. Recurrent pneumothorax related to diffuse dendriiform pulmonary ossification in genetically predisposed individual. *Respirol Case Rep* 2016;5:e00211.
 29. Matsuo H, Handa T, Tsuchiya M, et al. Progressive Restrictive Ventilatory Impairment in Idiopathic Diffuse Pulmonary Ossification. *Intern Med* 2018;57:1631-6.
 30. Uehara S, Udagawa N, Mukai H. Protein kinase N3 promotes bone resorption by osteoclasts in response to Wnt5a-Ror2 signaling. *Sci Signal* 2017. doi: 10.1126/scisignal.aan0023.
 31. Adzhubei IA, Schmidt S, Peshkin L, et al. A method and server for predicting damaging missense mutations. *Nat Methods* 2010;7:248-9.
 32. Ng PC, Henikoff S. SIFT: Predicting amino acid changes that affect protein function. *Nucleic Acids Res* 2003;31:3812-4.
 33. Schwarz JM, Cooper DN, Schuelke M, et al. MutationTaster2: mutation prediction for the deep-sequencing age. *Nat Methods* 2014;11:361-2.
 34. Shihab HA, Gough J, Cooper DN, et al. Predicting the functional, molecular, and phenotypic consequences of amino acid substitutions using hidden Markov models. *Hum Mutat* 2013;34:57-65.
 35. Lee HK, Chaboub LS, Zhu W, et al. Daam2-PIP5K is a regulatory pathway for Wnt signaling and therapeutic target for remyelination in the CNS. *Neuron* 2015;85:1227-43.
 36. Liu Y, Lusk CM, Cho MH, et al. Rare Variants in Known Susceptibility Loci and Their Contribution to Risk of Lung Cancer. *J Thorac Oncol* 2018;13:1483-95.
 37. Hirata H, Hinoda Y, Nakajima K, et al. Wnt antagonist gene polymorphisms and renal cancer. *Cancer* 2009;115:4488-503.
 38. Galamb O, Kalmar A, Peterfia B, et al. Aberrant DNA methylation of WNT pathway genes in the development and progression of CIMP-negative colorectal cancer. *Epigenetics* 2016;11:588-602.
 39. Zhu W, Krishna S, Garcia C, et al. Daam2 driven degradation of VHL promotes gliomagenesis. *Elife* 2017. doi: 10.7554/eLife.31926.
 40. Cui Q, Xie P. Correlation Between Daam2 Expression Changes and Demyelination in Guillain-Barre Syndrome. *Cell Mol Neurobiol* 2016;36:683-8.

41. Ajima R, Bisson JA, Helt JC, et al. DAAM1 and DAAM2 are co-required for myocardial maturation and sarcomere assembly. *Dev Biol* 2015;408:126-39.
42. Green JD, Harle TS, Greenberg SD, et al. Disseminated pulmonary ossification. A case report with demonstration of electron-microscopic features. *Am Rev Respir Dis* 1970;101:293-8.
43. Reinehr M, Rittinger M, Muller-Wening D, et al. Diffuse pulmonary ossifications with mortal consequences. A case report. *Pathologe* 2003;24:114-8.
44. Maiti SK, Singh GR. Bone morphogenetic proteins - Novel regulators of bone formation. *Indian J Exp Biol* 1998;36:237-44.
45. Mahy PR, Urist MR. Experimental heterotopic bone formation induced by bone morphogenetic protein and recombinant human interleukin-1B. *Clin Orthop Relat Res* 1988;236-44.
46. Akagawa KS, Takasuka N, Nozaki Y, et al. Generation of CD1+RelB+ dendritic cells and tartrate-resistant acid phosphatase-positive osteoclast-like multinucleated giant cells from human monocytes. *Blood* 1996;88:4029-39.
47. Agarwal S, Loder S, Brownley C, et al. Inhibition of Hif1alpha prevents both trauma-induced and genetic heterotopic ossification. *Proc Natl Acad Sci U S A* 2016;113:E338-47.
48. Mitchell EJ, Canter J, Norris P, et al. The genetics of heterotopic ossification: insight into the bone remodeling pathway. *J Orthop Trauma* 2010;24:530-3.
49. Chen YJ, Chang WA, Huang MS, et al. Identification of novel genes in aging osteoblasts using next-generation sequencing and bioinformatics. *Oncotarget* 2017;8:113598-613.
50. Kaplan FS, Xu M, Seemann P, et al. Classic and atypical fibrodysplasia ossificans progressiva (FOP) phenotypes are caused by mutations in the bone morphogenetic protein (BMP) type I receptor ACVR1. *Hum Mutat* 2009;30:379-90.
51. Regard JB, Malhotra D, Gvozdenovic-Jeremic J, et al. Activation of Hedgehog signaling by loss of GNAS causes heterotopic ossification. *Nat Med* 2013;19:1505-12.
52. Amalfitano M, Fyfe B, Thomas SV, et al. A case report of mesenteric heterotopic ossification: Histopathologic and genetic findings. *Bone* 2018;109:56-60.

Cite this article as: Sun SW, Zhou M, Chen L, Wu JH, Meng ZJ, Miao SY, Han HL, Zhu CC, Xiong XZ. Whole exome sequencing identifies a rare variant in *DAAM2* as a potential candidate in idiopathic pulmonary ossification. *Ann Transl Med* 2019;7(14):327. doi: 10.21037/atm.2019.06.14

Supplementary

Table S1 Pulmonary function variations over more than 2 years

Variables	2015-05-07	2017-07-28
VC (% predicted)	72	71.2
FRC (% predicted)	94	86
RV (% predicted)	106	94
TLC (% predicted)	76.7	60
FVC (% predicted)	74.4	72
FEV1 (% predicted)	65	63
FEV1/FVC (%)	74.3	73
PEF (% predicted)	77.9	93
PEF 25%	34	62
PEF 50%	45.4	48
PEF 75%	55	32
MVV (% predicted)	84.2	76
DLCO (% predicted)	66.3	61
RV/TLC (%)	139.4	101.7

The comparison shows slightly worsened restricted pulmonary ventilation dysfunction. VC, vital capacity; FRC, functional residual capacity; RV, residual volume; TLC, total lung capacity; FVC, forced vital capacity; FEV1, forced expiratory volume in 1 s; PEF, peak expiratory flow rate; MVV, maximum ventilatory volume; DLCO, carbon monoxide diffusion capacity.

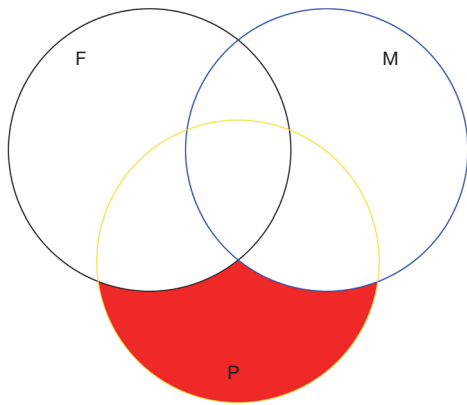


Figure S1 Exclusive filter strategy.

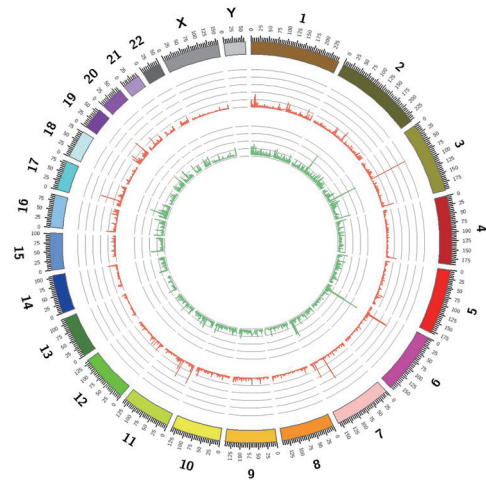


Figure S2 Overview of the variants, including SNVs and indels detected in the patient. SNVs, single nucleotide variants.

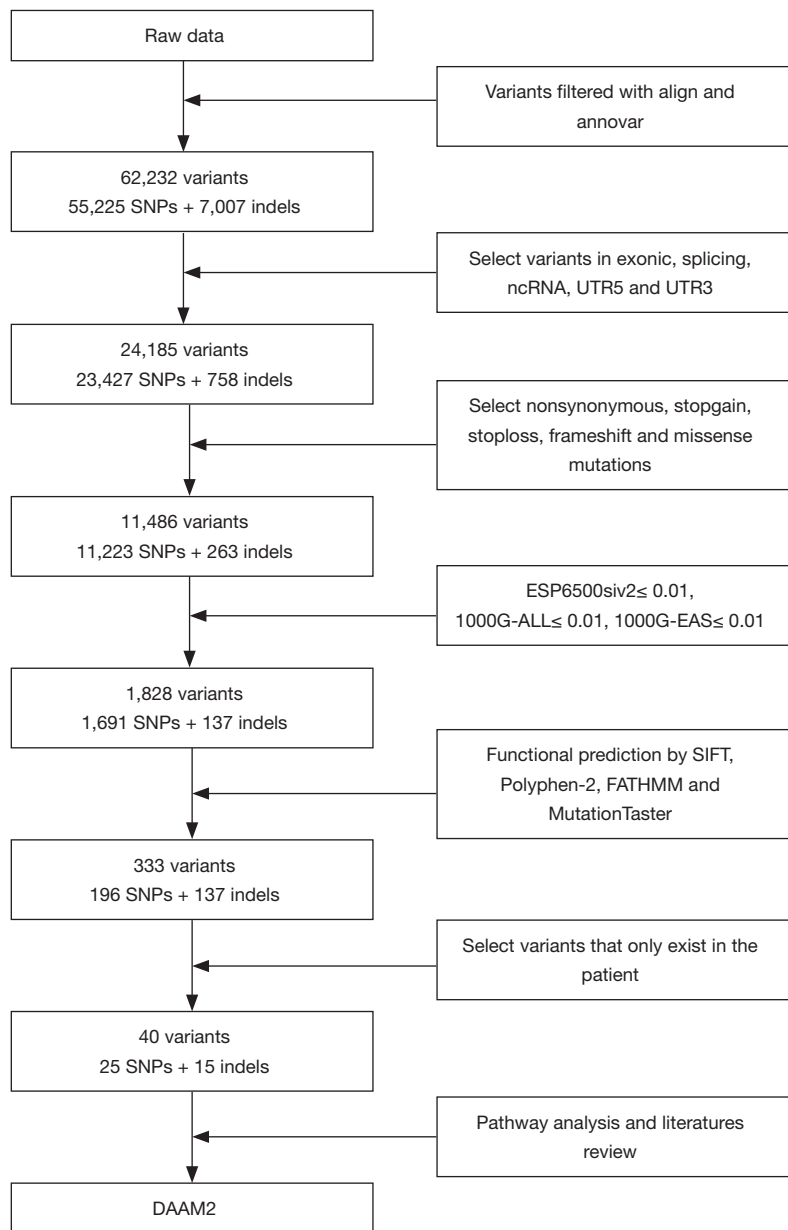


Figure S3 Flow chart for variant filtering used in the study.

Table S2 Information about the 40 candidate variants

Chr	Pos	Ref	Alt	Gene	SIFT	Polyphen-2	Mutation Taster	FATHMM	Mutant Frequency [†]	AA change
2	100210334	CG	C	AFF3	-	-	-	-	0.04081	A⇒fs
3	195505787	CGTGA	C	MUC4	-	-	-	-	0	G⇒fs
3	195507206	T	LFB [‡]	MUC4	-	-	-	-	0	S⇒fs
3	75790783	G	LFB [‡]	ZNF717	-	-	-	-	0.08824	S⇒fs
4	4190576	C	G	OTOP1	0	D	D	T	0.00002755	R⇒P
6	39869226	G	T	DAAM2	0	D	D	-	0.00004980	R⇒L
6	168376882	G	GT	HGC6.3	-	-	-	-	0	Q⇒fs
6	168376880	T	TG	HGC6.3	-	-	-	-	0	Q⇒fs
6	33167055	G	T	RXRB	0.01	D	D	D	0	P⇒Q
7	143453661	T	G	CTAGE6	-	-	-	-	0	E⇒A
7	100550485	A	G	MUC3A	-	-	-	-	0	S⇒G
7	100550486	G	T	MUC3A	-	-	-	-	0	S⇒I
7	100550488	A	T	MUC3A	-	-	-	-	0	M⇒L
7	100550507	C	T	MUC3A	-	-	-	-	0	T⇒I
7	100550570	T	C	MUC3A	-	-	-	-	0	M⇒T
7	100550571	G	C	MUC3A	-	-	-	-	0	M⇒I
7	100550602	T	A	MUC3A	-	-	-	-	0	S⇒T
7	149509455	C	T	SSPO	-	-	-	-	0.001	Q⇒X
8	7830694	C	A	USP17L8	-	-	-	-	0	A⇒S
11	99690482	C	LFB [‡]	CNTN5	-	-	-	-	0.01393	F⇒ANX
11	35640807	C	A	FJX1	0.01	D	D	T	0	P⇒Q
12	112036823	G	T	ATXN2	-	P	D	T	0	Q⇒K
12	58220811	G	T	CTDSP2	0	D	D	T	0	L⇒I
12	58220816	A	G	CTDSP2	0	P	D	T	0	I⇒T
12	53343231	G	C	KRT18	0	D	D	D	0	A⇒P
12	11420391	LFB [‡]	T	PRB3	-	-	-	-	0.1654	P fs
12	11420334	LFB [‡]	G	PRB3	-	-	-	-	0.1072	P⇒fs
13	78272267	T	TGG	SLAIN1	-	-	-	-	1	A⇒Q
14	20181609	T	C	OR11H2	-	-	-	-	0	Y⇒C
15	28518114	TC	T	HERC2	-	-	-	-	0	G⇒fs
15	22082368	G	C	POTEB2	-	-	-	-	0	Q⇒E
16	70977799	A	LFB [‡]	HYDIN	-	-	-	-	0	S⇒fs
16	28074466	C	A	GSG1L	0	D	D	T	0	D⇒Y
17	45234490	C	LFB [‡]	CDC27	-	-	-	-	0	E⇒fs
19	55370551	TGG	T	KIR3DL2	-	-	-	-	0	W⇒fs
19	55370554	C	CAT	KIR3DL2	-	-	-	-	0	P⇒fs
19	9006737	G	A	MUC16	0	D	D	T	0	L⇒F
19	18279974	A	G	PIK3R2	0	D	D	D	0.0002	Y⇒C
22	22989594	G	C	GGTLC2	-	-	-	-	0.0001587	R⇒P
22	22989602	C	T	GGTLC2	-	-	-	-	0	P⇒S

[†], data from GnomAD (East Asian); LFB[‡], large fragment base. Chr, chromosome; Pos, position; Ref, reference sequence base; Alt, alternative base identified; AA change, amino acid changes; D, probably damaging (Polyphen-2) or disease causing (MutationTaster and FATHMM); P, possibly damaging; T, tolerated.